

# Topology-Selective Chromatography Reveals Plasmid Supercoiling Shifts during Fermentation and Allows Rapid and Efficient Preparation of Topoisomers\*\*

Marek Mahut, Elisabeth Haller, Parisa Ghazidezfuli, Michael Leitner, Andreas Ebner, Peter Hinterdorfer, Wolfgang Lindner, and Michael Lämmerhofer\*

Plasmid DNA (pDNA) holds great potential for use in gene therapy and DNA vaccines. Therefore much attention has been paid to the biotechnological production of novel drugs of this type as they enter clinical evaluation. Herein we present a unique liquid-chromatography-based method for the efficient separation of topoisomers of the covalently closed circular (ccc) plasmid DNA, which is considered by the U.S. Food and Drug Administration to be therapeutically the most active isoform.<sup>[1]</sup> The separation relies on quinine-carbamate ligands on a silica support which cause the ccc isoform to split into a Gaussian distribution of discrete narrow peaks each corresponding to a discrete supercoiled species. The absolute supercoiling of single topoisomers isolated from the HPLC eluent was assigned by capillary gel electrophoresis. The analysis of in-process control samples taken during fermentation using 2D HPLC revealed a substantial change in the topoisomer pattern during upstream processing. Because of the high loadability of quinine-carbamate columns, this method is very useful for the preparative isolation of topoisomers with a desired degree of supercoiling.

The natural ccc isoform is a mixture of topoisomers each with a different degree of negative supercoiling. Briefly, DNA supercoiling is mathematically described by the linking number difference  $\Delta Lk$  between a given ccc topoisomer  $i$ ,  $Lk_i$ , and its standard state,  $Lk_0$ . The linking number  $Lk_i$  is an integer, which cannot be altered by mechanical deformation of the molecule.<sup>[2]</sup>  $Lk_0$  is calculated as the ratio between the

plasmid size  $N$  in base pairs (bp) and the helical repeat  $h$ , that is, the number of bp per turn of the double helix. Under standard conditions (0.2 M NaCl, pH 7, 37 °C),<sup>[3]</sup> the value 10.5 bp/turn is usually taken for B-DNA as  $h^0$  and  $Lk_0 = N/h^0$  (for a given pDNA with 4896 bp,  $Lk_0 = 466$ ). Geometrically, supercoiling consists of two quantities, twist (i.e. the coiling of the DNA strands around each other or around the axis of the DNA helix) and writhe (i.e. the coiling of the helix axis in space). For a successful separation strategy, it is necessary to specifically recognize either the superhelical turn moiety (writhe), or the distance between proximate base-pair moieties in the manner of groove-binding agents, or else the distance between adjacent nucleobases in the case of intercalators (both recognizing the twist).

Because writhe recognition would intuitively require a large selector, and intercalators show slow association and dissociation kinetics<sup>[4]</sup> resulting in broad peaks,<sup>[5]</sup> we have decided to design a low-molecular-weight selector that is able to recognize proximate structures in the DNA grooves. For this reason we have chosen a quinine-carbamate selector, where the distance between the tertiary amine and the carbamate moiety mimics some DNA-groove binders,<sup>[6]</sup> whose binding mode has been well characterized.<sup>[7]</sup> In addition to this basic structural motif being responsible for the chemically-driven geometrical differentiation, the hetero-aromatic group adds conformational stability to the molecule, as has been shown in our previous NMR studies.<sup>[8]</sup> The chromatographic stationary phase containing the mentioned selector can be seen in Figure 1 a.

Free quinine was previously shown to have intercalating properties;<sup>[9]</sup> therefore we studied whether the quinine-carbamate selector is also an intercalator and thus capable of changing the twist and hence the writhe of pDNA, which would interfere with the separation process. When we recorded atomic force microscopic (AFM) images of highly compacted pDNA according to our previously described method,<sup>[10]</sup> its shape did not change upon addition of *n*-butylcarbamoylquinine, which mimicks the chromatographic selector. However, after addition of chloroquine to the same solution, the plasmid structures relaxed, showing that quinine carbamate does not behave like an intercalator (Figure 1). Its binding mechanism is more along the lines of groove binding, in course of which DNA conformation does not change significantly from a macroscopic viewpoint.

A chromatographic separation of various plasmids of different sizes from different sources is shown in Figure 2 a–f, where each band represents a single topoisomer in its native

[\*] Dr. M. Mahut, Mag. E. Haller, Mag. P. Ghazidezfuli, Prof. W. Lindner, Prof. M. Lämmerhofer  
Institut für Analytische Chemie  
Universität Wien, Währinger Strasse 38, 1090 Wien (Austria)  
E-mail: Michael.Laemmerhofer@univie.ac.at

Dipl.-Ing. M. Leitner, Dr. A. Ebner, Prof. P. Hinterdorfer  
Institut für Biophysik, Johannes Kepler Universität  
Altenbergerstrasse 69, 4040 Linz (Austria)

Prof. P. Hinterdorfer  
Center for Advanced Bioanalysis (CBL)  
Gruberstrasse 40–42, 4040 Linz (Austria)

Prof. M. Lämmerhofer  
New address: Pharmazeutisches Institut, Universität Tübingen  
Auf der Morgenstelle 8, 72070 Tübingen (Germany)

[\*\*] We thank Boehringer-Ingelheim RCV (Vienna, Austria) for financial support and for providing plasmid material and fermentation samples. We also thank Andreas Reininger for help with AFM images.

Supporting information for this article is available on the WWW under <http://dx.doi.org/10.1002/anie.201106495>.

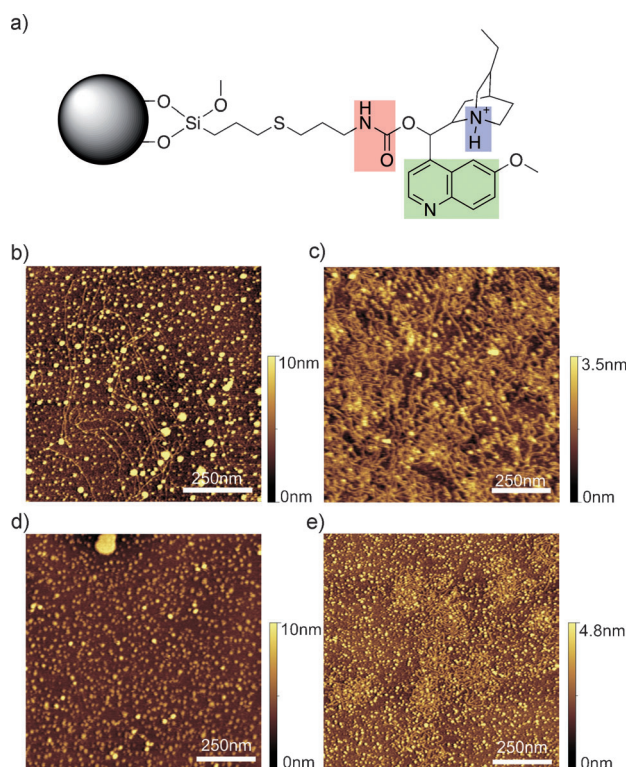


**Figure 1.** a) Quinine-carbamate (QC) ligand attached to silica through a thioether linker employed in topology-selective chromatography. AFM images of the highly compacted pMCP1 plasmid were recorded in liquid phase on APTES mica. After addition of the intercalator chloroquine (CLQ), the plasmid nanoparticles start to relax (b) (10 min after CLQ addition) until most of the double-strands are visible (c) (30 min after CLQ addition). After addition of QC, there is no macroscopic change in the shape of the plasmid nanoparticles (d) (30 min after QC addition). However, upon further addition of CLQ, the plasmid particles relax (e) (20 min after addition of CLQ).

form. Previously, such topoisomer distributions could be analyzed by electrophoretic techniques only.<sup>[11a,b]</sup> Although partial separation for simple supercoiled ccc plasmid topoisomers was found on an RP-18 column,<sup>[12]</sup> this was not a targeted selectivity and no resolution between adjacent native pDNA topoisomers could be achieved. Hence we report the first chromatographic deconvolution of a natural distribution of supercoiled plasmid topoisomers. We refer to our method as “topology analysis”; however, here we point out that other authors have used this term or a similar one for the separation of DNA isoforms meaning the three forms—linear, open circular, and covalently closed circular—which are not topological isomers in a strict sense.

To confirm the identity of the separated species, the peak areas of adjacent peaks were plotted in an  $x, y$  diagram for the plasmids pMCP1 and pAcMC1 with sizes of 4.9 kbp and 9.9 kbp, respectively, and subsequently fitted to a Gaussian function, using Equation (1) with  $a$ ,  $b$ , and  $x_0$  (Figure 2g, h) to be fitted.

$$f(x) = a \exp \left[ -\frac{1}{2} \left( \frac{x - x_0}{b} \right)^2 \right] \quad (1)$$

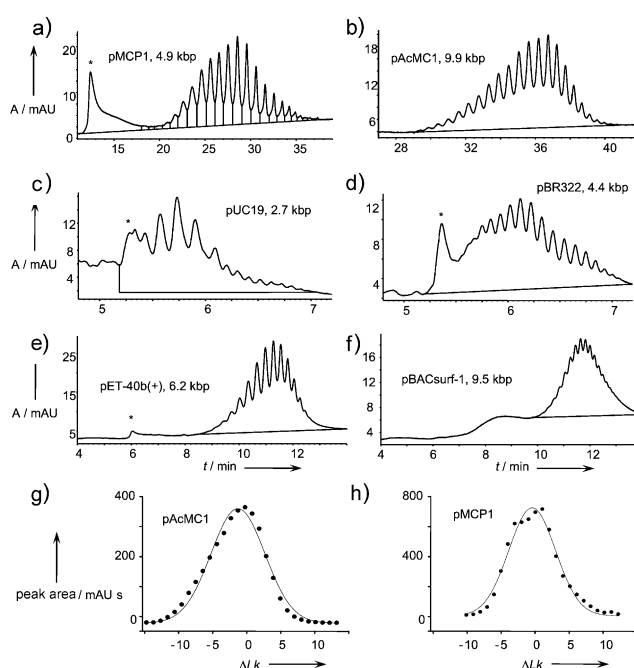


**Figure 2.** Various noncommercial (a,b) and commercial (c–f) plasmid preparations separated on the stationary phase shown in Figure 1a. The ccc forms of all plasmids could be separated into topoisomers, showing the universal applicability of the method, while the oc isoform is marked with an asterisk. In  $x, y$  diagrams adjacent topoisomer-peak areas are plotted against the linking number difference in relation to the most abundant topoisomer for the pMCP1 (g), data from (a), and pAcMC1 (h), data from (b) plasmid. The highest abundant topoisomer is set to  $\Delta Lk = 0$ . The overlaid curve is a fit to a Gaussian function as described in the text ( $R^2 = 0.989$  and  $0.990$ , respectively). (“A” means absorbance measured at 258 nm, “mAU” means milli absorbance units.)

Here,  $x_0$  is the small angular displacement<sup>[13]</sup> and  $-0.5 < x_0 < +0.5$  is valid. The curve fittings show a very good correlation, indicating that the peak areas follow a Maxwell–Boltzmann distribution. This can be easily rationalized since the free energies of the individual topoisomers are close, and correspondingly the probabilities of their existence are similar. In general, supercoiling introduces a torsional strain, meaning that the free energies of supercoiled topoisomers are higher, and thus these structures are energetically less favorable than relaxed pDNA.

Next, we preparatively isolated individual topoisomers by collecting column eluates of individual bands after UV detection. After concentration in a gentle stream of nitrogen gas and subsequent dialysis to remove a large part of salts, the eluates were rechromatographed using the same conditions as those used for fractionation. The eluates hereupon yielded discrete peaks and appeared at the retention time of their initial collection. In Figure 3, an overlay of a preparative chromatographic separation of a ccc pDNA together with three isolated fractions is shown. The elution order is the reverse of that from electrophoresis, which was confirmed by analysis of these fractions by capillary gel electrophoresis (see the Supporting Information). For complete characterization of the separated topoisomers, we determined the number of superhelical turns and linking number difference of fraction X

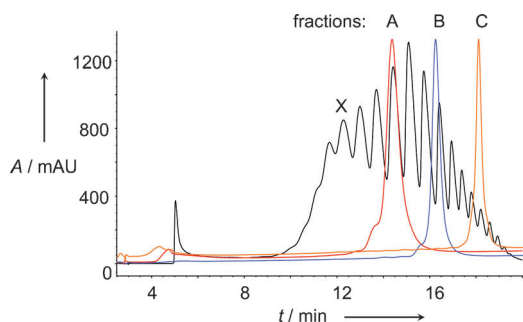


**Figure 3.** Chromatogram of a semipreparative run after injection of 285  $\mu$ g pMCP1 onto a topology-selective column, during which four fractions were isolated. From each of the isolated aliquots A, B, and C, a 20  $\mu$ L sample was re-injected individually and the corresponding chromatograms overlaid in the diagram (y axes were aligned). Fraction X was used for determination of the number of superhelical turns.

shown in Figure 3. We applied the Keller's band-counting method<sup>[14]</sup> and found that fraction X contains a topoisomer with  $\Delta Lk = -26 \pm 2$ . Following Figure 3 and the rule that topoisomers with higher supercoiling elute later from the chromatographic column, fractions A, B, and C have following numbers of negative superhelical turns:  $29 \pm 2$  (A),  $32 \pm 2$  (B),  $36 \pm 2$  (C). Finally it can be deduced that the topoisomer distribution in the natural sample of the pMCP1 plasmid is centered around the topoisomer with a mean linking difference  $\Delta Lk$  of  $-30 \pm 2$ , which corresponds to a superhelical density of  $-0.06$ , the mean value found in natural plasmids.<sup>[15]</sup> By convention, the standard error of the determined linking number using the agarose gel electrophoresis (AGE) method equals the number of gels employed, that is, two in this case (see the Supporting Information).

It has to be added that once such a topoisomer is characterized for a certain plasmid, it can serve as a reference point for future analyses. In semipreparative runs analytical columns have shown excellent loading capacities: 285  $\mu$ g pDNA was loaded in a single injection on a  $120 \times 4.0$  mm column containing a 5  $\mu$ m porous (120  $\text{\AA}$ ) material and no overloading effects were observed (Figure 3). Thus, sufficient quantities can be produced in short time for analytical purposes as individual topoisomer standards if required by regulatory bodies.

The current U.S. FDA guidelines for industry recommends that isoforms other than ccc

(linear and oc), RNA, proteins, and possibly harmful organic compounds should be monitored in final products. In the pharmaceutical industry, bulk quantities of pDNA are usually produced in large fermenters by *E. coli*, where the plasmids are amplified during fermentation (upstream process) and harvested in a multistep lysis and purification (downstream) process.<sup>[16]</sup> Samples drawn during the fermentation of pMCP1, and a smaller variant pMCP1-3.5 (3.5 kbp) lacking the antibiotic resistance gene, were subjected directly to topology analysis. On account of the significant contamination of the lysed cell mass samples with RNA, genomic DNA, and cell proteins, we employed a two-dimensional chromatography method, in which pDNA was isolated in the first dimension by size-exclusion chromatography (SEC) employing a porous (1000  $\text{\AA}$ ) silica-based SEC column. The pDNA peak eluting after 2 min was then transferred to the topology-selective quinine-carbamate column (for details see the Supporting Information).

The sequential injection of all fermentation samples allowed a direct comparison of the peak pattern by an overlay of the chromatograms (Figure 4a). In these overlays, the most abundant peak (highest area) of the topoisomer pattern is a good estimate of the mean plasmid supercoiling at time of sample drawing; therefore its position in the chromatogram was plotted against the duration of fermentation. A substantial change of topology in the course of the

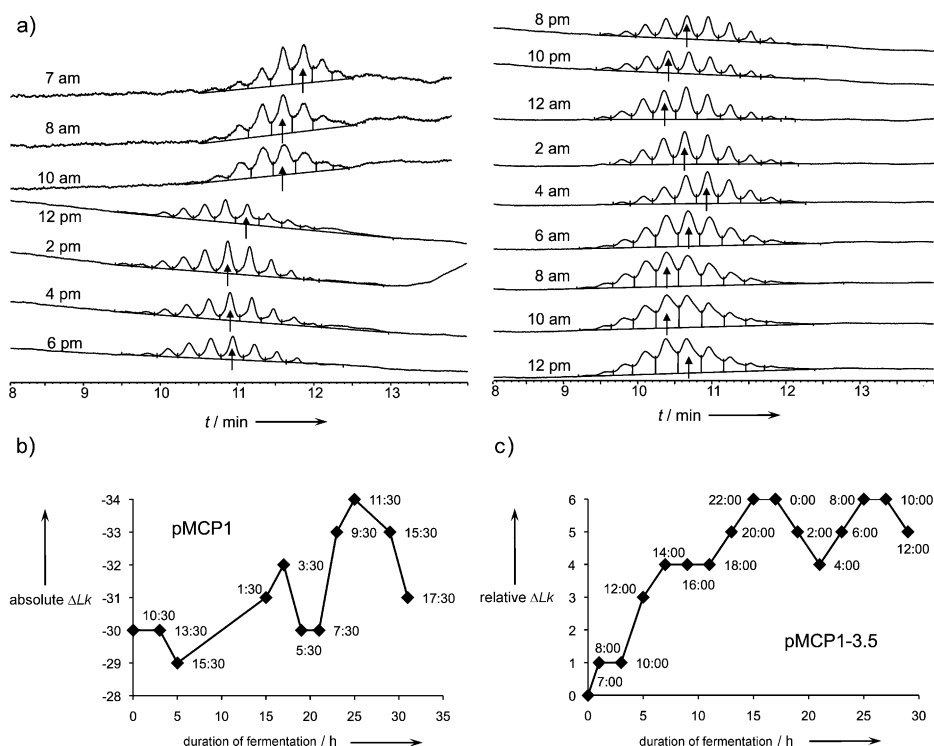


**Figure 4.** a) The overlay shows a series of samples drawn consecutively during a 30 h long fermentation of a pMCP1-3.5 plasmid in *E. coli* in intervals of two hours, analyzed by 2D-HPLC. The arrow indicates the most abundant topoisomer by peak area and hence the mean plasmid supercoiling. The insets show the actual daytime during sample drawing. The linking number of the most abundant topoisomer has been plotted against the fermentation duration of the pMCP1 (b) plasmid (supercoiling is given in absolute linking numbers, assigned by gel electrophoresis) and of the pMCP1-3.5 (c) (here the linking number is relative, the initial value was arbitrarily set to zero).

upstream process was observed for both plasmids. However, the supercoiling of the small pDNA decreased dramatically compared to the initial state, as indicated by the decrease of chromatographic retention, in the first hours (corresponding to the lag phase), while it remained similar towards the end of the fermentation (Figure 4b). The pMCP1 plasmid showed different behavior, because the initial and the final mean supercoiling were similar, but there were considerable shifts during the process (Figure 4c). This indicates that the cells' plasmid supercoiling responds differently to the conditions of fermentation between various plasmids, and interestingly, the topoisomer pattern may shift dramatically in the course of pDNA manufacturing relative to that of the initial bacterial strain. This change in topology is likely linked in our case to cell aging or the number of cell cycles. Interestingly, a circadian rhythm, which has been studied on the cyanobacterium *Synechococcus elongates* using AGE containing chloroquine,<sup>[17]</sup> may potentially superimpose the observed trends in plasmid topology. As expected, a change in plasmid supercoiling did not occur during downstream processing when we analyzed samples during individual cleaning steps because of lacking enzymatic activity.

We have shown that a quinine-carbamate stationary phase can be used to selectively separate the topoisomers of covalently closed circular plasmids; this is supplemented by fast binding and dissociation processes, as the chromatographic selector does not have potentially troublesome intercalating properties. The migration order is inverted relative to that of electrophoresis. Finally, the topology of fermentation samples of two different plasmid preparations was determined using a two-dimensional setup consisting of size-exclusion and topology-selective chromatography and was found to change considerably during fermentation.

## Experimental Section

For chromatographic analysis a mixed gradient of salt and 2-propanol from 0 to 100% B in 15 min (Figures 2c–f and 4) or 60 min (Figures 2a,b and 3) was used. Buffer A consisted of 50 mmol L<sup>-1</sup> NaH<sub>2</sub>PO<sub>4</sub> titrated to pH 7.0 with 5 M NaOH. Buffer B consisted of 50 mmol L<sup>-1</sup> NaH<sub>2</sub>PO<sub>4</sub>, 0.6 mol L<sup>-1</sup> NaCl, and 10% (v/v) 2-propanol titrated to pH 7.0 with 5 M NaOH. Between the analytical runs, the column was washed with a salt solution (injection of 50 µL 3 M NaCl (aq.)), followed by reequilibration at 0% B for 5 min. The flow rate

was set to 0.7 mL min<sup>-1</sup>, detection wavelength to 258 nm, and the temperature to 60 °C (solvent preheating).

Received: September 14, 2011

Published online: November 16, 2011

**Keywords:** cinchona alkaloids · DNA structures · liquid chromatography · molecular recognition · plasmid topoisomers

- [1] *Guidance for Industry: Considerations for Plasmid DNA Vaccines for Infectious Disease Indications*, U.S. Department of Health and Human Services, Food and Drug Administration, Rockville, MD, **2007**.
- [2] S. M. Mirkin, *Encyclopedia of Life Sciences* **2001**, 1–11.
- [3] W. R. Bauer, *Annu. Rev. Biophys. Bioeng.* **1978**, 7, 287–313.
- [4] R. R. Monaco, *J. Nucleic Acids* **2010**, 2010, 4.
- [5] T. Fornstedt, G. Zhong, G. Guiochon, *J. Chromatogr. A* **1996**, 742, 55–68.
- [6] a) R. Corradini, S. Sforza, T. Tedeschi, R. Marchelli, *Chirality* **2007**, 19, 269–294; b) J. B. Chaires, *Curr. Opin. Struct. Biol.* **1998**, 8, 314–320.
- [7] I. Haq, *Arch. Biochem. Biophys.* **2002**, 403, 1–15.
- [8] N. M. Maier, S. Scheffzick, G. M. Lombardo, M. Feliz, K. Rissanen, W. Lindner, K. B. Lipkowitz, *J. Am. Chem. Soc.* **2002**, 124, 8611–8629.
- [9] N. J. Pritchard, A. Blake, A. R. Peacocke, *Nature* **1966**, 212, 1360–1361.
- [10] M. Mahut, M. Leitner, A. Ebner, M. Lämmerhofer, P. Hinterdorfer, W. Lindner, *Anal. Bioanal. Chem.* **2011**, 1–8.
- [11] a) M.-D. Mayán-Santos, M.-L. Martínez-Robles, P. Hernandez, D. Krimer, J. B. Schwartzman, *Electrophoresis* **2007**, 28, 3845–3853; b) D. J. Clark, B. Leblanc, *Methods Mol. Biol.* **2009**, 543, 523–535.
- [12] U. Kapp, J. Langowski, *Anal. Biochem.* **1992**, 206, 293–299.
- [13] A. D. Bates, A. Maxwell in *DNA Topology*, 2nd ed., Oxford University Press, New York, **2006**.
- [14] W. Keller, *Proc. Natl. Acad. Sci. USA* **1975**, 72, 4876–4880.
- [15] W. R. Bauer, F. H. C. Crick, J. H. White, *Sci. Am.* **1980**, 243, 118–124; W. R. Bauer, F. H. C. Crick, J. H. White, *Sci. Am.* **1980**, 243, 126; W. R. Bauer, F. H. C. Crick, J. H. White, *Sci. Am.* **1980**, 243, 129–130; W. R. Bauer, F. H. C. Crick, J. H. White, *Sci. Am.* **1980**, 243, 132–133.
- [16] a) J. Urthaler, C. Ascher, H. Woehrer, R. Necina, *J. Biotechnol.* **2007**, 128, 132–149; b) J. Urthaler, W. Buchinger, R. Necina, *Acta Biochim. Pol.* **2005**, 52, 703–711.
- [17] M. A. Woelfle, Y. Xu, X. Qin, C. H. Johnson, *Proc. Natl. Acad. Sci. USA* **2007**, 104, 18819–18824.